Attenuation of conducted vasodilatation in rat mesenteric arteries during hypertension: role of inwardly rectifying potassium channels

Kenichi Goto, Nicole M. Rummery, T. Hilton Grayson and Caryl E. Hill

Division of Neuroscience, John Curtin School of Medical Research, Australian National University, Canberra, ACT, 0200, Australia

The present study was designed to elucidate whether the conduction of vasomotor responses mediated by endothelium-derived hyperpolarizing factor (EDHF) in rat mesenteric arteries is altered during hypertension. Iontophoresed acetylcholine (ACh; 500 ms) caused EDHF-mediated hyperpolarization and vasodilatation at the local site and these responses spread through the endothelium to remote sites in 12-week-old Wistar-Kyoto rats (WKY). Conducted responses were significantly attenuated in age-matched spontaneously hypertensive rats (SHR) although the rate of decay with distance did not change. Inhibition of inwardly rectifying potassium (Kir) channels (30 μM barium) eliminated the difference between WKY and SHR by attenuating conducted responses in WKY but not SHR. At the local site, barium (30 μM) significantly reduced the duration but not the amplitude of ACh-induced hyperpolarization in WKY only. Barium had no effect when the iontophoretic stimulus was reduced to 350 ms. After blockade of EDHF in SHR, ACh elicited a depolarization which our indirect data suggest spreads along the vessel in the endothelium. Messenger RNA expression of Kir2.0 genes did not differ between the strains nor did the amplitude of K^+-induced hyperpolarization, which was abolished by disruption of the endothelium. Immunohistochemistry revealed a decrease in connexin (Cx)37 but not Cx40 or Cx43 protein in endothelial cells of SHR compared to WKY. Results suggest that conduction of EDHF-mediated responses in WKY, but not in SHR, is facilitated by activation of Kir channels at the site of ACh application and not by differences in endothelial connexin expression. Lack of Kir channel involvement in hypertension may result from reduction in the duration of the hyperpolarization due to the development of ACh-mediated depolarization, rather than to any difference in Kir subunit expression or function.

(Received 21 June 2004; accepted after revision 1 October 2004; first published online 1 October 2004)
Corresponding author K. Goto: Division of Neuroscience, John Curtin School of Medical Research, Australian National University, Canberra, A.C.T., 0200, Australia. Email: kenichi.goto@anu.edu.au

Topical application of some vasodilator substances to the microcirculation induces a relaxation at the local site and this spreads rapidly to remote sites along the vessel wall (Duling & Berne, 1970). Although vasodilators, such as acetylcholine (ACh), stimulate several vasodilatory factors, including nitric oxide (NO), prostacyclin and endothelium-derived hyperpolarizing factor (EDHF), which contribute to the local response (Hill *et al.* 2001), recent studies suggest that EDHF is the key player responsible for conducted vasodilator responses in certain vascular beds (Welsh & Segal, 2000; Hoepfl *et al.* 2002).

Accumulating evidence suggests that the spread of electrical signals from endothelial to smooth muscle cells via gap junctions may account for EDHF in some vessels (Yamamoto *et al.* 1998; Coleman *et al.* 2001; Griffith *et al.* 2002; Sandow *et al.* 2002, 2004). Conducted responses attributed to EDHF also result from the electronic spread of current through gap junctions along the vessel wall in hamster cheek pouch arterioles (Segal & Duling, 1989). However, in hamster feed arteries, the length constant, or distance over which the response decays to 37% of its initial value, was increased when the hyperpolarization was initiated by ACh rather than by current injection (Emerson *et al.* 2002). This observation implies that regenerative mechanisms could be involved in the conducted hyperpolarization induced by ACh. Indeed some recent studies have suggested that a regenerative mechanism, probably involving the activation of inwardly rectifying (Kir) potassium channels, mediates agonist-induced conducted vasomotor response in certain microvascular beds (Rivers

 DOI: 10.1113/jphysiol.2004.070458

et al. 2001; Horiuchi *et al.* 2002; Crane *et al.* 2004), although no direct electrophysiological evidence of the involvement of Kir channels in the regenerative mechanism has been so far provided.

In hypertension, EDHF-mediated vasodilator responses are impaired (Fujii *et al.* 1992; Goto *et al.* 2000), as is the expression of connexins (Cx) (Rummery *et al.* 2002*a*; Kansui *et al.* 2004), which comprise gap junctions in the endothelial cell layer, through which vasodilator responses are conducted (Segal, 2001). Changes in K^+ channel function have also been reported in hypertension (Sobey, 2001). In particular, the function of Kir channels, which play an important role in the regulation of resting membrane potential and vascular tone (Quayle *et al.* 1997), is reduced in cerebral arteries from stroke-prone spontaneously hypertensive rats (McCarron & Halpern, 1990). These observations led us to hypothesize that the conduction of vasomotor responses may be attenuated during hypertension, owing to the reduction in the number of gap junctions and/or impairment of Kir channel function.

We have therefore examined whether conducted vasomotor responses, generated by EDHF, are altered in mesenteric arteries during hypertension. The branching nature of the mesenteric circulation, combined with the demonstration that vasodilatation can be conducted from a point source over large distances in these primary mesenteric vessels and in smaller tertiary arteries (Takano *et al.* 2004), suggests that these responses could play an important role in coordinating blood flow to considerable areas of the gut. Attenuation of the ability to conduct vasodilatation in these resistance arteries might therefore compromise gut function and contribute to increased peripheral vascular resistance.

Methods

All experiments were approved by the Australian National University Animal Experimentation Ethics Committee under guidelines of the National Health and Medical Research Council of Australia (NHMRC). Twelve-week-old male Wistar-Kyoto (WKY) and age-matched spontaneously hypertensive rats (SHR) were used. Systolic blood pressure was measured using tail-cuff plethysmography

Physiological experiments

Rats were anaesthetized with ether and killed by decapitation. A 10 mm segment of a primary mesenteric artery supplying the upper ileum was removed, cleaned of fat and pinned to the base of a recording chamber. In some preparations, the endothelium was selectively disrupted in one half of the segment length by gently rubbing the intimal surface with a human hair. Impairment of endothelial function was confirmed by the absence of ACh-mediated hyperpolarization. Tissues were superfused (3 ml min^{-1}) with Krebs solution (mmol l^{-1}): NaCl 120; KCl 5; $NaHCO_3$ 25; NaH_2PO_4 1; $CaCl_2$ 2.5; $MgCl_2$ 2; glucose 11; at 34–35°C, gassed with 95% O_2−5% CO_2. N^{ω}-Nitro-L-arginine methyl ester (L-NAME, 100 μmol l^{-1}) and indomethacin (10 μmol l^{-1}) were present in all experiments to inhibit NO and prostanoid production, respectively. Each preparation was taken from a different animal.

After equilibration for 40 min, membrane potentials of vascular smooth muscle cells were recorded with conventional microelectrodes (tip resistance, 120–240 MΩ) (Hill *et al.* 1999), containing 0.2% propidium iodide in 0.5 mol l^{-1} KCl for identification of impaled cells. Criteria for successful recordings for the electrophysiological experiments included the following: an abrupt drop in voltage when the vascular smooth muscle cell was impaled by the microelectrode, a stable impalement for at least 2 min, and a sharp return to zero potential upon withdrawing the electrode. Cells were impaled near the midpoint of the arterial segment and ACh (1 mol l^{-1}; 500 ms, 500 nA) iontophoresed from a micropipette (tip diameter ∼1 μm) and the change in membrane potential recorded. A retaining current (200 nA) was used to prevent continuous release of ACh from the pipette. The ACh pipette was then moved progressively to sites at 500, 1000, 1500, 2000, or 2500 μm downstream, with respect to the superfusion solution, from this measuring (0 μm) site and similar measurements made (Fig. 1*A*). The response to ACh was then studied again at the measuring (0 μm) site to verify the reproducibility of the hyperpolarization. Where possible, a complete series of measurements was made from the same cell

Identical experiments were conducted in the presence of 30 μmol l^{-1} barium, to specifically inhibit Kir channels (Quayle *et al.* 1997). Responses to ACh applied locally and 1000 μm downstream from the measuring (0 μm) site were also studied in the presence of apamin (0.5 μmol l^{-1}, small-conductance Ca^{2+}-sensitive K^+ channel, K_{Ca}, inhibitor) plus charybdotoxin (60 nmol l^{-1}, large and intermediate-conductance K_{Ca} inhibitor) or in arteries in which the endothelium was disrupted. The possibility of ACh diffusion to remote sites was tested by progressively raising the ejection micropipette away from the arterial surface (Fig. 2).

Membrane potential changes produced by bath applied K^+ (10–30 mmol l^{-1}) were measured in the presence or absence of barium (30 μmol l^{-1}). K^+ solutions were prepared by equimolar replacement of Na^+ with K^+. Experiments were carried out in the presence of nifedipine (1 μmol l^{-1}), as 30 mmol l^{-1} K^+ generated depolarization and constriction, which prevented stable impalements. The effect of K^+ on membrane potential was also tested in endothelium-disrupted arteries.

ACh-induced vasodilatation was measured using video microscopy and an edge-detection program (DIAMTRAK, ver. 5, T. O. Neild) (Neild, 1989) in similarly prepared arterial segments preconstricted with 1 μmol l^{-1} PE, which produced a submaximal constriction (60% of the maximum constriction to phenylephrine (PE)). Conducted responses were investigated in the presence and absence of barium (Fig. 3*A*).

For both hyperpolarization and relaxation, conducted responses at each point were expressed as a percentage of the initial response to ACh applied at the measuring (0 μm) site, to facilitate comparison of the slopes of decay. Both the peak response, as well as the area under the response curve (AUC, mV•s, μm•s) were measured to account for any changes in overall response duration. All chemicals were from Sigma (St Louis, MO, USA).

Expression of messenger RNA

Mesenteric arteries were removed from WKY and SHR, immersed in RNAlater (Ambion Inc., Austin, TX, USA) and extraneous material removed in cold phosphate-buffered saline (PBS). Samples ($n = 3$) comprised primary and secondary mesenteric arteries supplying the upper ileum, and each sample was taken from two animals. Samples of the adductor magnus muscle and cerebral cortex were used as positive controls for the expression of Kir2.1 and for Kir2.2, 2.3, and 2.4, respectively. Samples were snap frozen in liquid nitrogen and processed using the RNeasy Mini Kit (Qiagen Inc., Doncaster, Victoria, Australia), including a 20 min DNAse treatment. mRNA was reverse transcribed to cDNA (42°C 1 h, 50°C 1 h, 90°C 10 min) using oligo dT (500 ng μl^{-1}, Invitrogen, Mulsgrave, Victoria, Australia) primers and Superscript II (200 U μl^{-1}, Invitrogen). For every sample, reactions from which either reverse transcriptase or RNA was omitted were run in parallel to control for contaminating DNA.

PCR reactions were performed using specific primers for each member of the rat Kir2.0 subfamily (GenBank): Kir2.1 forward 5′-gcggtggatgctggtaatcttctg-3′ and reverse 5′-gacctcagacacacacgctttgct-3′ (136 bp; accession numbers AF021137, NM_017296), Kir2.2 forward 5′-tcgccaacatggatgagaagtcac-3′ and reverse 5′-atgacccagaagatgatgccgaac-3′ (145 bp; acc. nos NM_053981, X78461), Kir2.3 forward 5′-cctcatgagccaggaggaagaaga-3′ and reverse 5′-tcaagcatccggataatgcctgtc-3′ (120 bp; acc. nos U27582, NM_053870, XM_216984, X83580, X87635), and Kir2.4 forward 5′-ccatgactacacaatgccgctcat-3′ and reverse 5′-tacgttcggtggaagtgtcgatag-3′ (127 bp; acc. nos AJ003065, NM_1707181). Reaction mixtures (20 μl) contained 1 U AmpliTaq Gold polymerase, reaction buffer containing 3 mmol l^{-1} $MgCl_2$ (Applied Biosystems, Scoresby, Victoria, Australia), 5 pmol of each primer (Invitrogen), 1 mmol l^{-1} dNTPs and 25 ng cDNA template. Cycling conditions were 95°C, 10 min and 35 cycles of 95°C 30 s, 65°C 30 s and 72°C 60 s. Amplification of glyceraldehyde-3-phosphate dehydrogenase (GAPDH) was performed using rat-gene specific primers 5′-accacagtccatgccatcac-3′ and 5′-tccaccaccctgttgctgta-3′ (452 bp; acc. nos BC059110, X02231, AB017801, M17701) and cycling conditions were 95°C, 10 min and 35 cycles of 95°C 30 s, 55°C 30 s and 72°C 60 s. Products were identified on 2% agarose gels stained with ethidium bromide and confirmed by sequencing (ABI 3730 Capillary Genetic Analyser, Biomolecular Resource Facility, John Curtin School of Medical Research, ANU).

Quantitative PCR

Quantitative PCR was used to determine the absolute copy numbers of each Kir2.0 subtype in mRNA extracted from the mesenteric arteries of WKY and SHR rats ($n = 3$). The copy numbers were obtained using standard curves constructed by amplification of known quantities of plasmid DNA containing a cloned PCR product insert corresponding to each Kir2.0 subtype. Each 25 μl PCR reaction mixture was prepared using the SYBR Green Core Reagents kit (Applied Biosystems) and contained 1 μl of each primer (final concentration 800 nM), 2 μl of 12.5 mM dNTPs, 3 μl of 25 mM $MgCl_2$, 0.125 μl of AmpliTaq Gold (5 U μl^{-1}), 2.5 μl of 10 × SYBR Green buffer, 10.375 μl H_2O and 5 μl of template containing either 10 ng of cDNA or diluted plasmid DNA containing the relevant cloned PCR product. All samples were diluted in water containing tRNA (2 ng μl^{-1}). All reactions were performed in duplicate using the ABI Prism 7700 Sequence Detection System (Applied Biosystems) at 95°C for 10 min, and 40 cycles of 20 s at 95°C, 20 s at 65°C, 45 s at 72°C. Every experiment included duplicate control reactions containing the corresponding untranscribed RNA sample, and water and the expression of all of the genes was determined in every sample. The integrity of each PCR reaction was checked using dissociation curve analysis after every reaction.

For each gene, the absolute mRNA concentration was determined by comparing the fluorescence signal at threshold (equal to 10 × S.D. of baseline fluorescence) to that generated by a standard curve using serial dilutions (from ~10^5 to 11 copies) of a known concentration of purified plasmid DNA containing the relevant cloned PCR product. The concentration of each Kir2.0 mRNA was normalized by comparison with 18S rRNA concentration, which was determined by using primers complementary to a region of the 5′ end of the molecule and a standard curve using serial dilutions of plasmid DNA containing the cloned fragment of the 18S rRNA gene (Rummery *et al.* 2002*b*).

Immunohistochemistry

Rats were anaesthetized with ketamine/rompun (44/8 mg kg^{-1} I.P.) and perfused with 0.9% NaCl

Table 1. Baseline characteristics and local response to acetylcholine in mesenteric artery of WKY and SHR

	Control			+ Barium		
	WKY	SHR	*n*	WKY	SHR	*n*
Resting membrane potential (mV)	−51 ± 1	−50 ± 1	22	−48 ± 1*	−47 ± 1*	11
Resting diameter (μm)	364 ± 13	385 ± 11	8	402 ± 15	387 ± 14	8
Response to acetylcholine						
Hyperpolarization (mV)	−17 ± 1	−15 ± 1	10	−17 ± 1	−14 ± 1	11
AUC (mV•s)	263 ± 43	156 ± 13†	7	170 ± 15*	151 ± 11	7
Dilatation (μm)	26 ± 3	32 ± 4	8	29 ± 2	31 ± 4	8
AUC (μm•s)	121 ± 25	146 ± 31	8	109 ± 15	130 ± 25	8

Values are means ± S.E.M. *$P < 0.05$ *versus* corresponding strain control; †$P < 0.05$ *versus* WKY.

containing 0.1% $NaNO_3$, 0.1% BSA and 5 U ml^{-1} heparin, followed by 2% paraformaldehyde in 0.1 mol l^{-1} sodium phosphate. Mesenteric arteries were removed and cut open longitudinally.

Whole-mount preparations were blocked in 2% BSA, 0.2% Triton X-100/PBS (30 min) and incubated in affinity purified sheep anti-Cx37, Cx40, or Cx45 (Rummery *et al.* 2002*b*) or rabbit anti-Cx43 (Zymed Laboratories, Inc. San Francisco, CA, USA; 1 : 100 in blocking buffer, 2 h, 37°C). Staining was visualized with Cy3-conjugated anti-rabbit or anti-goat immunoglobulins (1 : 100 in 0.01% Triton X-100/PBS, 1 h, room temperature (RT); Jackson ImmunoResearch Laboratories, Inc., West Grove, PA, USA). Some samples were subsequently incubated with rabbit anti-human von Willebrand factor (anti-vWF, 1 : 300, 1 h, RT; Dako Cytomation, Botany, NSW, Australia), followed by swine anti-rabbit FITC (1 : 40, 1 h, RT, Dako) to detect endothelial cells.

To test for specificity, tissues were incubated either without primary antibody or with primary antibody previously pre-incubated (l h, RT) with a 10-fold excess by weight of the antigenic peptide. Confocal pictures of these controls (Fig. 11*A*) were obtained using the same pinhole and voltage settings as those used for preparations incubated with primary antibodies which had been pre-incubated in PBS without antigenic peptide. For Cx43 staining, there was no FITC labelling if anti-vWF was not present.

Samples were viewed using a Leica confocal microscope (TCS 4D, Leica Microsystems, Gladesville, NSW, Australia), with argon–krypton laser. Optical sections were collected at 1 μm intervals throughout the endothelial cell layer, as determined by the extent of the anti-vWF labelling, and the series recombined into a singe image. Similar gain settings were used for comparisons of antibody staining between vessels.

Morphometric measurements of endothelial cells and Cx expression within the endothelium were made on recombined images (Analytical imaging station, Imaging Research, Inc., St Catharines, Ontario, Canada). For each animal, at least three composite images were analysed and arteries taken from four different animals. Endothelial cells labelled for Cx37 were used to determine cell length, width, area and perimeter. Cx expression was quantified by measuring the average size of the smallest labelled structures in each preparation and defining these as individual gap junctional plaques. Cx density was determined using the grain counting function. The number of Cx plaques per 100 μm of endothelial cell perimeter was calculated using the endothelial cell parameters.

Statistical analysis

Data were expressed as means ± S.E.M.; *n* refers to the number of animals examined. Statistical significance was determined by one-way or two-way ANOVA followed by Fisher's *post hoc* test for multiple comparisons, or by paired and unpaired Student's *t* test, as appropriate. A level of $P < 0.05$ was considered statistically significant.

Results

Body weight was similar between the strains (259 ± 4 g, WKY, $n = 10$; 262 ± 3 g, SHR, $n = 12$; $P > 0.05$). Systolic blood pressure was significantly higher in SHR than in WKY (199 ± 5 *versus* 127 ± 4 mmHg, respectively; $P < 0.05$; $n = 4$–5).

Conduction of hyperpolarization

All cells impaled were confirmed by dye labelling to be smooth muscle cells. Resting membrane potential did not differ between the strains (Table 1). At the site of application, ACh produced a hyperpolarization in both strains (Fig. 1*B*, 0 μm). The amplitude of this hyperpolarization did not differ between the strains although the overall response (AUC) was significantly smaller in SHR compared with WKY (Table 1). ACh-induced hyperpolarization spread upstream in both strains. The conducted-response curves decayed at similar rates as a function of distance ($P > 0.05$), but the WKY

curve had a plateau region near the point of ACh application which caused a significant rightward shift compared with the SHR curve (Fig. 1*C*). When ACh was re-applied at the measuring (0 μm) site at the end of the experiments, no significant changes in ACh-induced hyperpolarization were observed (Fig. 1*C*). Withdrawing the ACh-micropipette away from the artery progressively reduced the local response, which was < 5 mV when the separation was > 250 μm and completely abolished when the separation was 500 μm (Fig. 2).

Conduction of vasodilatation

The resting diameter of the mesenteric arteries without PE did not differ between SHR and WKY (Table 1) and incubation with PE produced a similar constriction in both strains (WKY 296 ± 12 μm; SHR 304 ± 18 μm, $n = 8$). At the measuring (0 μm) site, ACh produced a vasodilatation, which was occasionally followed by oscillation in both strains (Fig. 3*B*). The amplitude and AUC of the vasodilatation did not differ significantly between the strains (Table 1). ACh-induced vasodilatation spread upstream, with respect to the superfusion solution, along the vessel in both strains. Both curves had plateau regions near the point of ACh application, although the plateau region of the WKY extended further, resulting in a significant rightward shift of its decay phase (Fig. 3*C*). The slope of the decay with distance was not significantly different between the strains ($P > 0.05$). The reproducibility of ACh-induced vasodilatation was verified by application of ACh at the

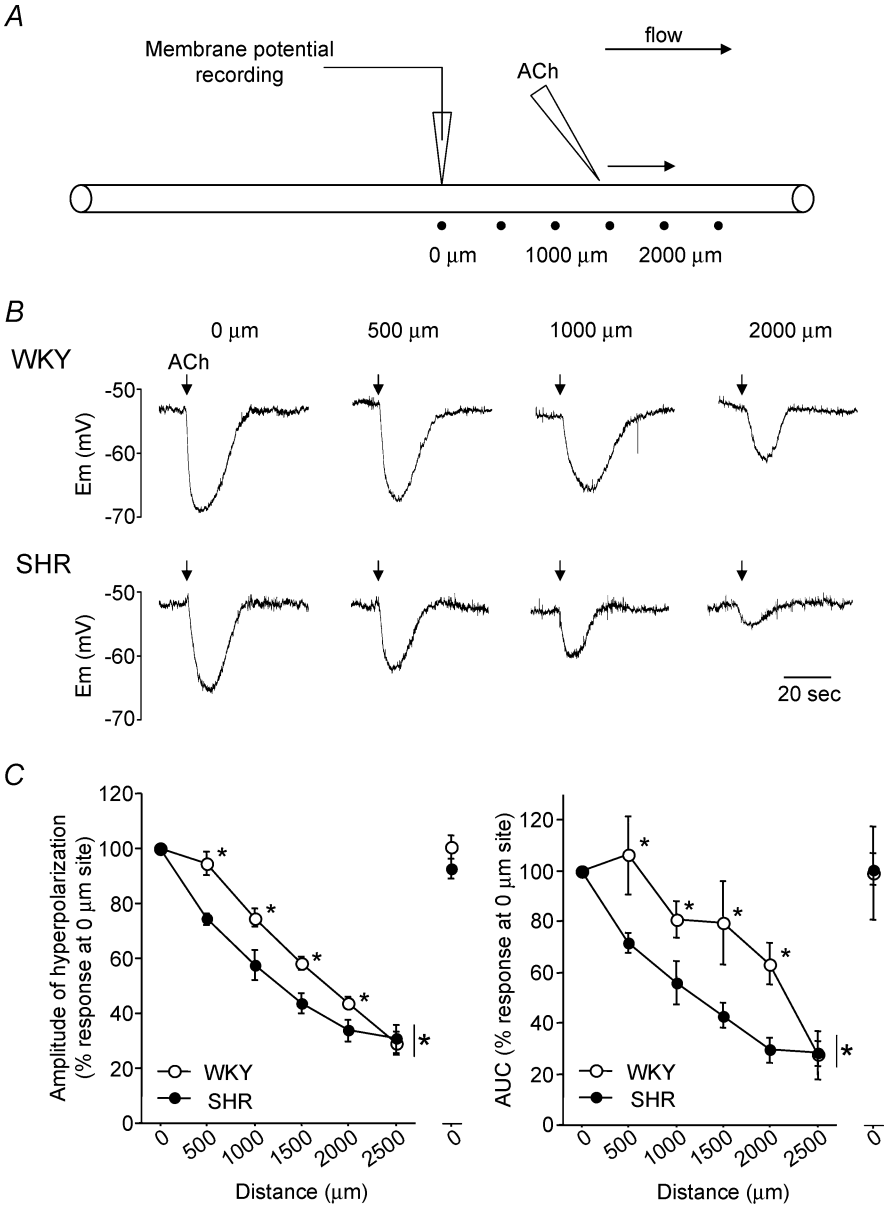

Figure 1. Conduction of hyperpolarization in WKY and SHR
A, ACh (1 mol l^{-1}; 500 ms, 500 nA) was iontophoresed at the measuring (0 μm) site and at 500, 1000, 1500, 2000 or 2500 μm downstream from the measuring site and then again at the measuring site. Smooth muscle cells were impaled at the midpoint of the arterial segment. Representative tracings (*B*) and summarized data (*C*) of conducted hyperpolarization. The amplitude and area under the conducted-response curve (AUC) were significantly shifted leftwards in SHR compared with WKY. Indomethacin (10 μmol l^{-1}) and L-NAME (100 μmol l^{-1}) present throughout. Representative tracings were obtained from the same cell in each strain. Data are means ± S.E.M.; $n = 7$ in each strain. *$P < 0.05$ *versus* WKY. Bar at the end of the data indicates statistical significance between the group data.

measuring (0 μm) site at the end of the experiments (Fig. 3*C*).

Effect of barium on conducted vasomotor responses

Inhibition of Kir channels with barium (30 μmol l^{-1}) significantly depolarized the membrane in the two strains, but did not alter resting vessel diameter (Table 1). At the ACh application site (0 μm), barium did not alter the vasodilatory response to ACh although the overall hyperpolarization (AUC) was significantly reduced in WKY but not in SHR (Table 1). In WKY, the conducted-response curves for hyperpolarization (Fig. 4*A* and *B*) and vasodilatation (Fig. 4*C* and *D*) were shifted leftwards by barium. In contrast, barium failed to shift the conducted-response curves in SHR (Fig. 4). In the presence of barium, there was no significant difference either in conducted hyperpolarization or conducted vasodilatation between the strains (Fig. 4).

When the relationship between the AUC for hyperpolarization and the AUC for relaxation was tested in both WKY and SHR, in the presence or absence of barium, a significant linear correlation was found ($P < 0.05$), although the goodness of fit was better for SHR ($r^2 = 0.85$) and for either WKY or SHR in the presence of barium (WKY/Ba $r^2 = 0.92$, SHR/Ba $r^2 = 0.89$), than it was for WKY ($r^2 = 0.72$). When the relationship between the AUC for hyperpolarization and the AUC for relaxation was only considered for points where the AUC for hyperpolarization was greater than 175 mV•s, as was the case in WKY, there was no significant correlation between the two parameters ($P = 0.82$).

Effect of $[K^+]_o$ on membrane potential

Raising $[K^+]_o$ from 5 (Krebs solution) to 30 mmol l^{-1} hyperpolarized the membrane in a concentration-dependent manner and the amplitude of K^+-induced hyperpolarization did not differ between the strains (maximal hyperpolarization, -6 ± 1 mV, WKY, $n = 5$; -7 ± 1 mV, SHR, $n = 5$; $P > 0.05$; Fig. 5*A* and *B*). In some preparations, 20 mmol l^{-1} $[K^+]_o$ and in all preparations, 30 mmol l^{-1} $[K^+]_o$, produced a subsequent depolarization (20 mmol l^{-1}: 2 ± 1 mV, WKY, $n = 5$; 0 ± 0 mV, SHR, $n = 5$; $P < 0.05$; 30 mmol l^{-1}: 9 ± 1 mV, WKY, $n = 5$; 6 ± 1 mV, SHR, $n = 5$; $P > 0.05$). In both strains, barium (30 μmol l^{-1}) abolished the K^+-induced hyperpolarization (Fig. 5*A* and *B*) without affecting K^+-induced depolarization (20 mmol l^{-1}: 2 ± 1 mV, WKY, $n = 4$; 1 ± 0 mV, SHR, $n = 4$; $P > 0.05$; 30 mmol l^{-1}: 7 ± 2, WKY, $n = 4$; 6 ± 1 mV, SHR, $n = 4$; $P > 0.05$).

Expression of Kir2.0 genes

Messenger RNAs corresponding to Kir2.1, 2.2 and 2.4 but not 2.3 were expressed in mesenteric arteries. Using the methods for the amplification of each specific Kir2.0 subunit that we have carefully designed and tested, in both strains, Kir2.2 appeared to be more abundant

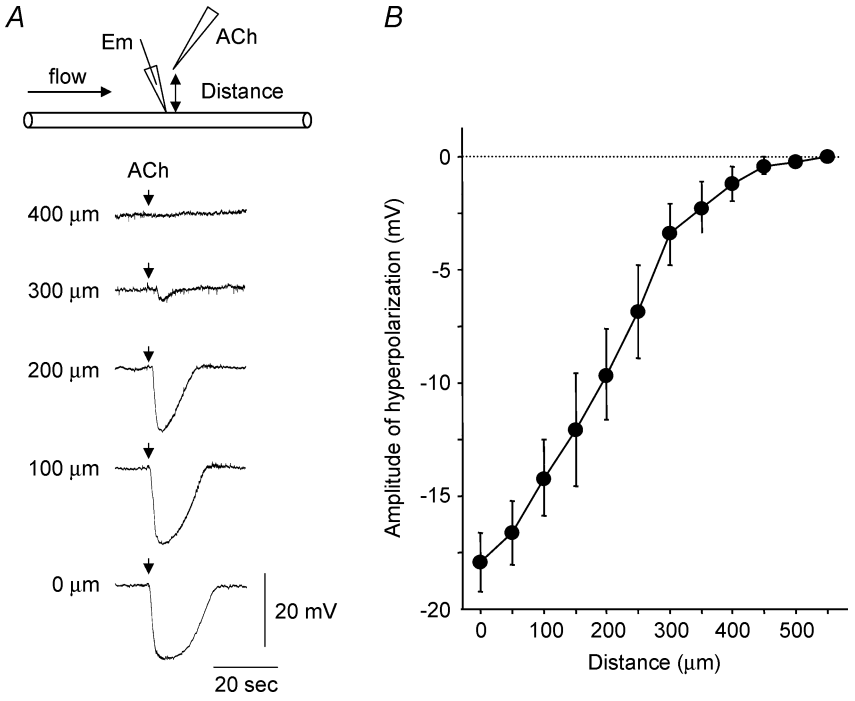

Figure 2. Effect of retraction of the iontophoretic micropipette away from the arterial surface on ACh-induced hyperpolarization
Representative tracings (*A*) and summarized data (*B*). Retracting the ejection micropipette ~500 μm away from the artery abolished the ACh-induced hyperpolarization at the local site. Representative tracings were obtained from the same cell. Data are means ± S.E.M.; $n = 7$.

than Kir2.1 and Kir2.4 (Fig. 5*C*). All four subtypes were strongly expressed in the positive control tissues of skeletal muscle (Kir2.1) and brain (Kir2.2, 2.3, and 2.4). The DNA sequences of each PCR product matched that of the corresponding Kir2.0 channel subfamily member to which complementary primers were designed. The experiment was studied using three distinct samples for each strain of rat with the same result. The amplification of GAPDH shows a closely similar level of expression of this constitutively expressed house-keeping enzyme between the samples.

Quantitative PCR

The absolute mRNA concentration in each unknown sample was determined from a standard curve using serial dilutions of purified plasmid DNA containing the relevant cloned PCR product (Fig. 6). To correct for variations in the overall efficiency of the reactions, the copy numbers for each subtype were normalized to the number of copies of 18S rRNA and were expressed as copies/10^6 copies of 18S rRNA (Table 2). This work confirmed the findings presented in Fig. 5*C* and showed that within the mesenteric arteries of 12 week WKY and SHR, the relative expression

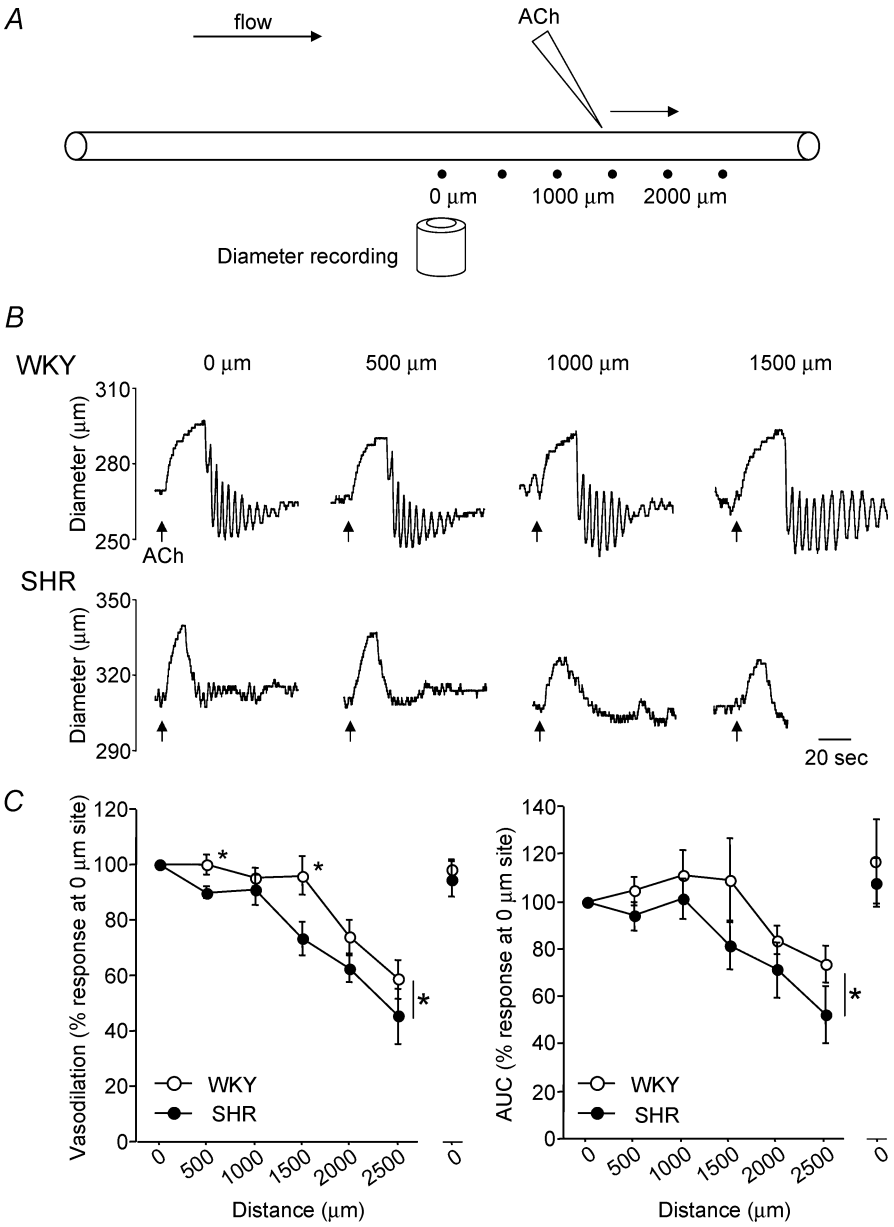

Figure 3. Conduction of vasodilatation in WKY and SHR
A, ACh (1 mol l^{-1}; 500 ms, 500 nA) was iontophoresed at the measuring (0 μm) site and at 500, 1000, 1500, 2000, or 2500 μm downstream from the measuring site and then again at the measuring site. Diameter change was recorded at the midpoint of the arterial segment. Representative tracings (*B*) and summarized data (*C*) of conducted vasodilatation. The amplitude and area under the conducted-response curve (AUC) were significantly shifted leftwards in SHR compared with WKY. Indomethacin (10 μmol l^{-1}) and L-NAME (100 μmol l^{-1}) present throughout. Representative tracings were obtained from the same preparation in each strain. Data are means ± S.E.M.; $n = 8$ in each strain. *$P < 0.05$ *versus* WKY. Bar at the end of the data indicates statistical significance between the group data.

was Kir2.2 > Kir2.4 > Kir2.1. For each subtype, there was no significant difference in expression between WKY and SHR ($P > 0.05$). Dissociation curve analysis confirmed the presence of a single amplicon in each reaction (Fig. 6).

Role of the endothelium in K^+-induced hyperpolarization

Disruption to the endothelium did not alter the resting membrane potential in both strains (-50 ± 1 mV, WKY, $n = 8$; -49 ± 1 mV, SHR, $n = 8$). In the endothelium-intact arteries, bath applied K^+ produced robust hyperpolarization in both strains (Fig. 7*A* and *C*). By contrast, in the endothelium-disrupted arteries, K^+-induced hyperpolarization was abolished in both strains (Fig. 7*B* and *C*). At higher concentration of K^+ (20 mmol l^{-1}), a depolarization was recorded in both strains (Fig. 7*A*–*C*).

ACh-induced depolarization

The combination of apamin plus charybdotoxin significantly depolarized the membrane in both strains (3 ± 1 mV, WKY, $n = 8$; 3 ± 1 mV, SHR, $n = 8$). Subsequent application of ACh at the measuring site produced membrane depolarization which was significantly larger in SHR than in WKY and the depolarization spread to a distant (1000 μm) site in both strains (Fig. 8*A* and *B*).

Role of the endothelium in conducted vasomotor responses

Impairment of endothelial function in half of the arterial segment did not alter the membrane potential in either strain (– endothelium -50 ± 1 mV, WKY; -51 ± 1 mV, SHR; + endothelium -51 ± 1 mV, WKY; -49 ± 1 mV, SHR; $n = 5$, $P > 0.05$). In the endothelium-intact half of the artery, ACh applied at the measuring site produced robust hyperpolarizing responses in both strains ($n = 5$ in each; Fig. 9*A* and *E*). By contrast, ACh applied at the measuring site in the endothelium disrupted half of the same arterial segments failed to produce a hyperpolarization in either strain ($n = 5$ in each; Fig. 9*B* and *E*). When ACh was applied 1000 μm

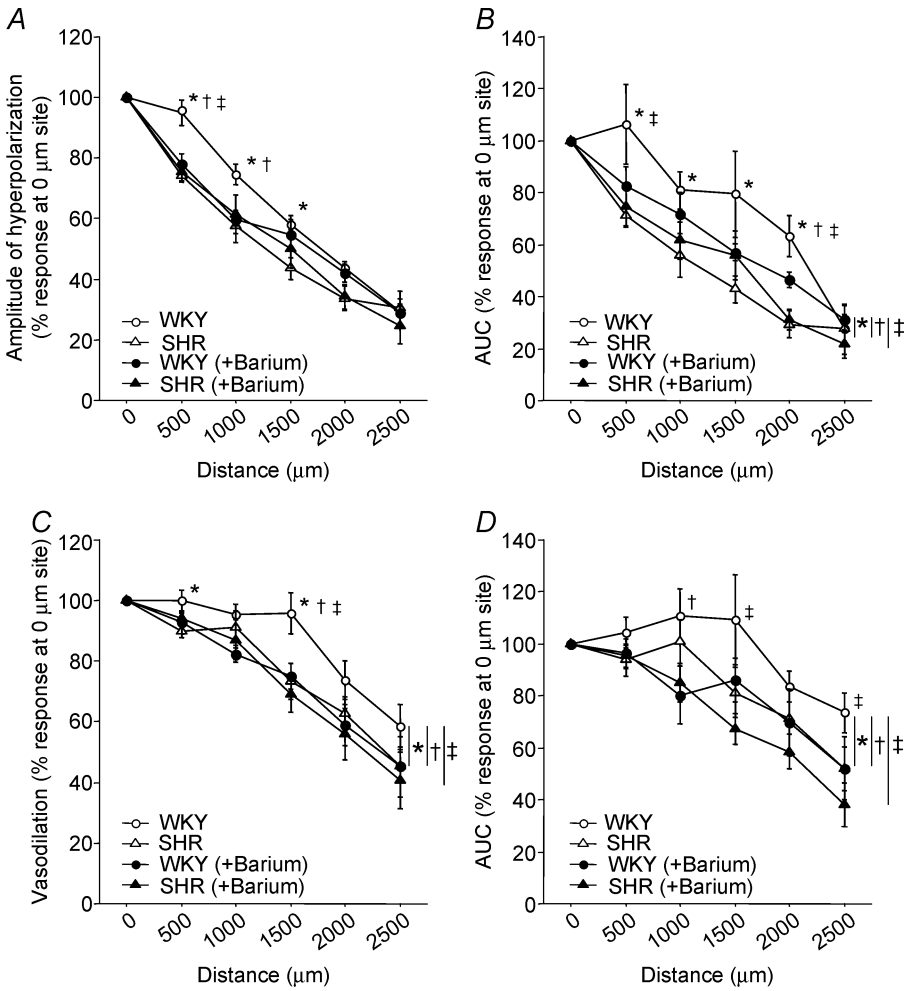

Figure 4. Effect of barium on conducted hyperpolarization and vasodilatation in WKY and SHR
In WKY, the amplitude and area under conducted-response curves for hyperpolarization (*A* and *B*) and vasodilatation (*C* and *D*) were shifted leftwards by barium. In contrast, barium failed to shift the conducted-response curves in SHR (*A*–*D*). In the presence of barium, there was no significant difference in conducted responses between the two strains (*A*–*D*). Data for WKY and SHR are repeated from Figs 1 and 3 for visual comparison. Indomethacin (10 μmol l^{-1}) and L-NAME (100 μmol l^{-1}) present throughout. Data are means ± S.E.M.; $n = 7$ (*A* and *B*) and 8 (*C* and *D*) in each strain. *$P < 0.05$ WKY *versus* SHR; †$P < 0.05$ WKY *versus* WKY (+ Barium); ‡$P < 0.05$ WKY *versus* SHR (+ Barium). Bars at the end of the data indicate statistical significance between the different group data.

downstream from the measuring site, hyperpolarization was recorded when the endothelium was intact ($n = 7$, Fig. 9*C* and *E*), but not when the endothelium in the intervening region had been damaged in both strains ($n = 5$, Fig. 9*D* and *E*).In the presence of charybdotoxin and apamin to block the hyperpolarization, ACh produced a depolarization in the endothelium-intact half of the artery in SHR, indicating that impairment to endothelial function did not interfere with the generation of depolarization in the intact portion (Fig. 9*A*). When ACh was applied to the endothelium-disrupted half of arterial segments in the absence of charybdotoxin and apamin, neither hyperpolarization nor depolarization was recorded (Fig. 9*B*). Depolarization was also not recorded from the endothelium-disrupted half of the artery when ACh was applied to the endothelium-intact half of the same arterial segment, suggesting that the depolarization generated in the intact segment could not be conducted in the smooth muscle (Fig. 9*A* and *D*).

In the endothelium-disrupted half of the artery, vasoconstrictor responses to PE ($1\ \mu mol\ l^{-1}$) were preserved in both strains (resting diameter: WKY, 348 ± 16 *versus* $285 \pm 16\ \mu m$ for $-$PE and $+$PE, respectively, $n = 8$, $P < 0.01$; SHR, 358 ± 13 *versus* $295 \pm 18\ \mu m$ for $-$PE and $+$PE, respectively, $n = 3$, $P < 0.05$) while vasodilator responses to ACh were absent in both strains (WKY, $1 \pm 1\ \mu m$, $n = 4$; SHR, $1 \pm 1\ \mu m$, $n = 3$). In the endothelium-intact half of the artery preconstricted with PE ($1\ \mu mol\ l^{-1}$), ACh applied at the measuring site produced robust vasodilatation in both strains (WKY; $30 \pm 3\ \mu m, n = 4$, SHR; $36 \pm 9\ \mu m, n = 3$). Like the hyperpolarization, these robust vasodilator responses did not conduct into the endothelium disrupted segment (WKY; $2 \pm 1\ \mu m$, $n = 4$, SHR; $0 \pm 0\ \mu m$, $n = 3$).

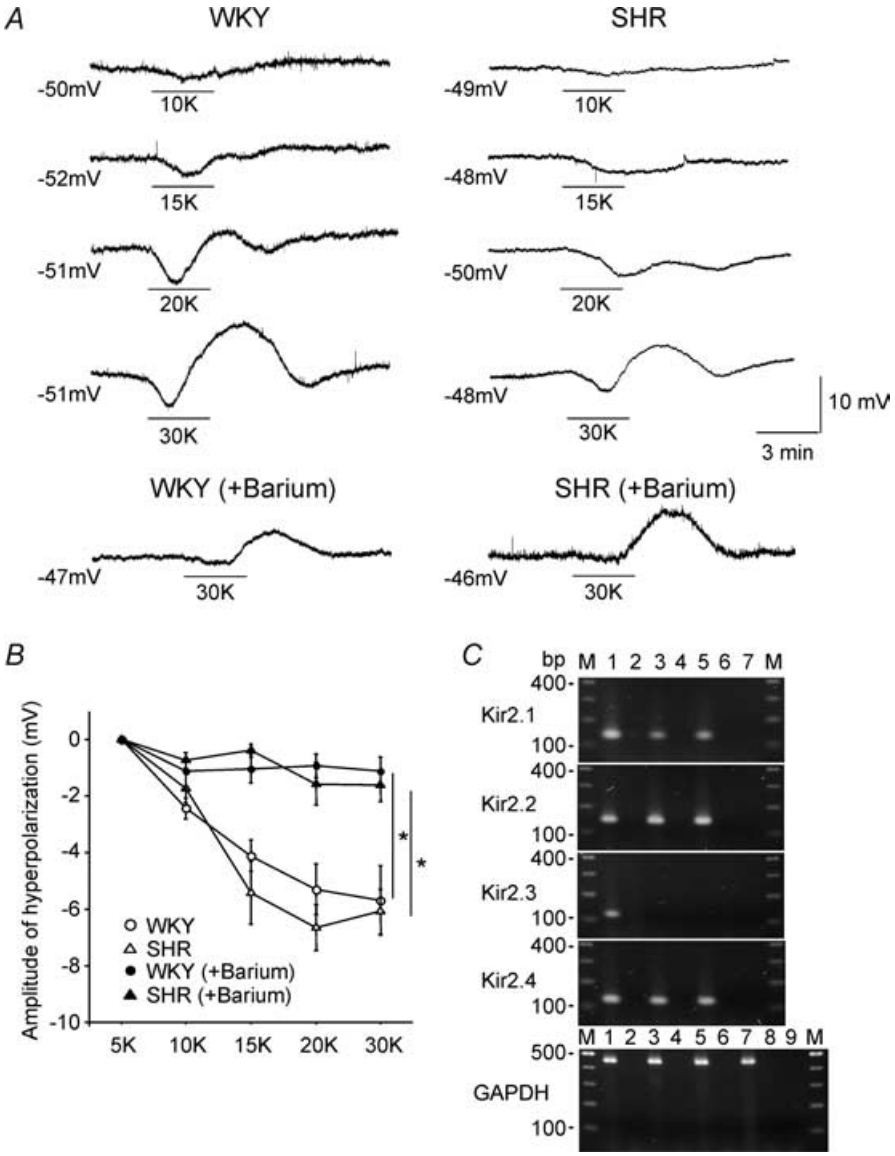

Figure 5. Effects of $[K^+]_o$ on membrane potential in WKY and SHR
Representative tracings (*A*) and summarized data (*B*). Bath-applied K^+ hyperpolarized the membrane to a comparable extent in the two strains and elicited depolarization at higher concentrations. Barium ($30\ \mu mol\ l^{-1}$) abolished K^+-induced hyperpolarization. Indomethacin ($10\ \mu mol\ l^{-1}$), L-NAME ($100\ \mu mol\ l^{-1}$) and nifedipine ($1\ \mu mol\ l^{-1}$) present throughout. Data are means ± S.E.M.; $n = 4$–5 in each strain. $^*P < 0.05$ *versus* without barium. *C*, expression of Kir2.0 subfamily members in WKY and SHR. Lane 1, + RT skeletal muscle (Kir2.1) or brain (Kir2.2–2.4); 2, – RT skeletal muscle (Kir2.1) or brain (Kir2.2–2.4); 3, + RT WKY mesenteric artery; 4, – RT WKY mesenteric artery; 5, + RT SHR mesenteric artery; 6, – RT SHR mesenteric artery; 7, control reverse transcription reaction without RNA; M, 100 bp ladder. + RT reactions contained RNA and Superscript II, – RT reactions contained RNA but no Superscript II. For GAPDH expression lane 1, + RT skeletal muscle; 2, − RT skeletal muscle; 3, +RT brain; 4, – RT brain; 5, + RT WKY mesenteric artery; 6, – RT WKY mesenteric artery; 7, + RT SHR mesenteric artery; 8, – RT SHR mesenteric artery; 9, control reverse transcription reaction without RNA

Role of hyperpolarization in the activation of Kir channels at the site of ACh application

The hyperpolarization to ACh applied at the measuring site was slower in onset in SHR than in WKY (Fig. 10*A*). When recordings were made from the same cell in SHR, after blocking the hyperpolarization with apamin plus charybdotoxin, the time course of the depolarization was found to be coincident with the hyperpolarization (Fig. 10*A*). In WKY, barium significantly reduced the AUC but did not alter the amplitude or onset of the hyperpolarization induced by ACh iontophoresed for 500 ms. However, when the ACh stimulus was shorter (350 ms), the AUC of the hyperpolarization, but not the amplitude, was significantly reduced and barium had no further effect (Fig. 10*B* and *C*). In SHR, the AUC of the hyperpolarization induced by ACh was significantly smaller than in WKY (Fig. 10*B* and *C*). Neither the AUC nor the amplitude of the hyperpolarization in SHR was affected by barium (Fig. 10*B* and *C*).

Endothelial cell morphology and Cx expression

Punctate staining for Cx37, 40 and 43, but not Cx45, delineated the endothelial cells in a similar manner in the mesenteric artery of both strains, although the cells were significantly smaller in SHR (Fig. 11*A* and *B*). In the absence of the primary antibody, no staining was observed with either the Cy3-conjugated

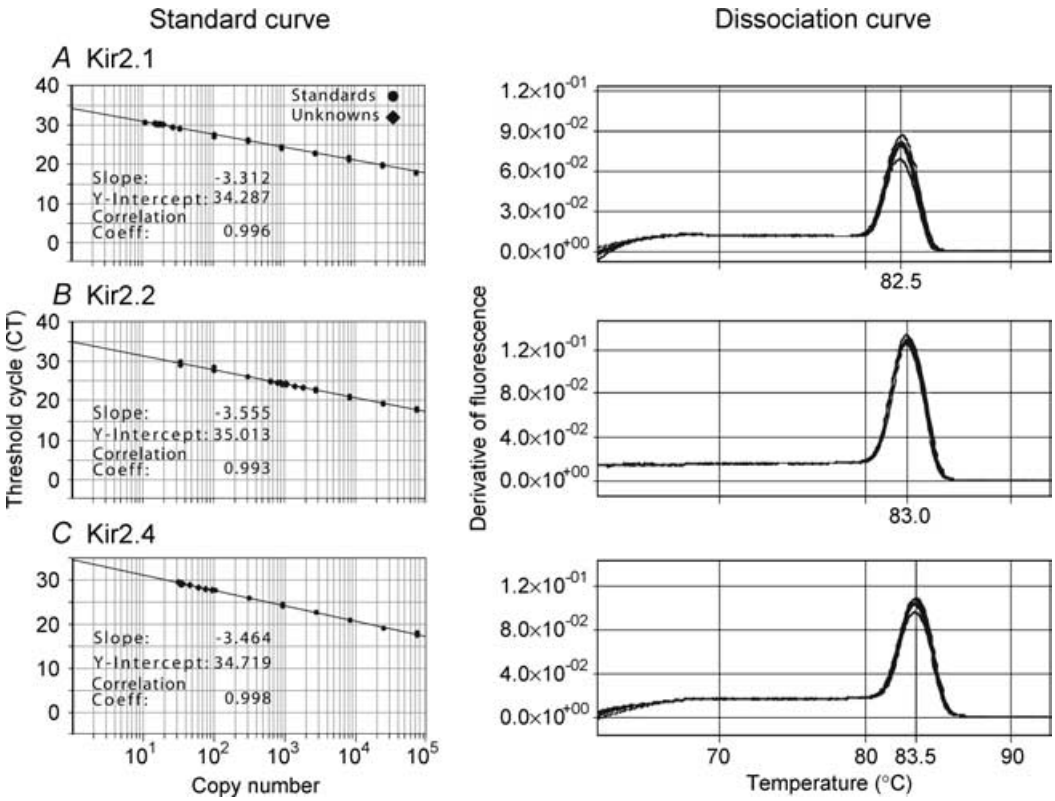

Figure 6. Standard curves and dissociation curve analysis was conducted for every sample following quantitative PCR using rat gene-specific primer sets to amplify Kir2.1 (*A*), Kir2.2 (*B*) and Kir2.4 (*C*) from WKY and SHR mesenteric artery

The standard curve for each specific rat Kir2.0 gene was generated using plasmid DNA of known concentration and copy number containing the cloned and sequenced PCR product. In the examples presented here, 'unknowns', representing duplicate reactions of three different WKY mesenteric artery samples ($n = 3$), were interpolated from the standard curves. The slope, *Y*-intercept and correlation coefficient of the standard curves were very similar demonstrating that these data closely matched the expected log-linear amplification relationship. Dissociation curve analysis of the same samples was conducted immediately following the amplification reactions and the rate of change of fluorescence with temperature was calculated and plotted as the derivative of fluorescence using the software supplied with the SDS7700 (Applied Biosystems). For each primer set, a single symmetrical peak of fluorescence can be seen in the dissociation curves for the six WKY samples, demonstrating the amplification of a single unambiguous product. The peak melting temperature for each gene product, 82.5°C for Kir2.1, 83.0°C for Kir2.2 and 83.5°C for Kir2.4, was similar to the predicted theoretical melting temperature estimated by computer software (82.44°C for Kir2.1, 82.21°C for Kir2.2 and 83.07°C for Kir2.4).

Table 2. Normalized copy number of mRNA for each Kir2.0 subtype (copies per 10^6 copies of 18S rRNA) expressed in mesenteric artery

Channel subtype	WKY	*n*	SHR	*n*
Kir2.1	33 ± 3	3	46 ± 3	3
Kir2.2	2548 ± 568	3	3006 ± 818	3
Kir2.4	134 ± 32	3	165 ± 37	3

Values are means ± S.E.M. *n* = number of RNA samples.

anti-goat or anti-rabbit immunoglobulins (Fig. 11*A* for Cy3-anti-goat). In addition, for each of the Cx antisera, there was no staining when the primary antibody was pre-incubated with the appropriate antigenic peptide (Fig. 11*A* for Cx37).

As Cx expression in the endothelium was seen exclusively around the cell periphery, the density of Cx plaques in the cell membrane was calculated to account for differences in endothelial size. The density of Cx37 plaques per 100 μm of endothelial cell perimeter was significantly less in SHR than in WKY, while there was no significant difference between plaque density for either Cx40 or Cx43 (Fig. 11*C*).

Discussion

The present study demonstrates that: (1) vasomotor responses can be conducted through the endothelium of primary mesenteric arteries of rats, (2) conduction of vasomotor responses is facilitated by Kir channel activation within the vicinity of the agonist application site in normotensive but not in hypertensive rats, and (3) there is an increase in endothelium-dependent depolarization in hypertensive rats and this may offset the augmentation by Kir channels.

In the presence of L-NAME and indomethacin, iontophoresed ACh produced hyperpolarization and vasodilatation both at the stimulation site and at remote upstream sites. Diffusion of ACh could not account for responses at the upstream sites, because retraction of the ejection micropipette ~500 μm away from the arterial surface eliminated the responses. Our results showed that the endothelium was essential for the generation and conduction of the EDHF-mediated hyperpolarization in rat mesenteric arteries, consistent with results in hamster feed arteries (Emerson & Segal, 2000), guinea-pig mesenteric arterioles (Yamamoto *et al.* 2001), and third order mesenteric arteries in rats (Takano *et al.* 2004). Since myoendothelial gap junctions exist in these vessels (Sandow & Hill, 2000; Sandow *et al.* 2003) and appear to play a critical role in EDHF responses (Sandow *et al.* 2002; Goto *et al.* 2002), it is reasonable to suggest that electrical signals generated at the stimulation site spread to the upstream sites through the endothelium and are then transmitted to neighbouring smooth muscle cells via myoendothelial gap junctions.

In the present study, the resting membrane potential was approximately 20 mV more negative than that reported for either arterioles or feed arteries studied previously. The difference may be explained by the experimental condition employed, i.e. vessels were pinned to the base of a recording chamber in the present study, whereas vessels were subjected to transmural pressure in previous studies. Indeed pressurization is reported to produce membrane depolarization of smooth muscle cells (Harder, 1984). However, the difference may not be simply explained by pressurization alone, because the membrane potential for pressurized rat resistance mesenteric arteries has been reported to be around −50 mV (Oishi *et al.* 2002), which is similar to the value of the present study. Alternatively, membrane properties might differ between large and small vessels. The diameter of the rat resistance mesenteric arteries (300–400 μm) used here was considerably larger than arterioles or feed arteries studied previously (10–100 μm).

This is the first study to demonstrate an alteration in conducted vasomotor responses in genetically hypertensive rats. In the present study, both the conducted-response curves for hyperpolarization and vasodilatation were shifted significantly leftwards in SHR compared with WKY. This shift appeared to be largely due to the presence of a more extended plateau region near the point of ACh application in WKY, rather than a change in the slope of decay of the responses with distance. Interestingly, a decrease in the overall hyperpolarization (AUC) at the ACh application site was seen in arteries from SHR, compared to WKY. Thus the difference in the spread of responses observed between the two strains appeared to result from changes occurring in the vicinity of the stimulation site rather than in the ability of the endothelium to conduct the hyperpolarization along the vessel length.

In mesenteric arteries of WKY, exposure to 30 μmol l^{-1} barium, a specific concentration to inhibit Kir channels (Quayle *et al.* 1997), caused a significant leftward shift in the conducted-response curves for both hyperpolarization and vasodilatation. While a contribution of Kir channels to agonist-induced conducted vasodilatation has also been reported in porcine coronary (Rivers *et al.* 2001) and rat cerebral penetrating arterioles (Horiuchi *et al.* 2002), our study is the first to measure effects on conducted hyperpolarization. The absence of an effect of Kir block on the slope of the decay of responses suggests that Kir channel involvement occurs in the vicinity of the ACh application, rather than at the more remote sites. This is consistent with the activation of Kir channels by the increase in extracellular K^+ ions (Quayle *et al.* 1997) as a result of the ACh-induced activation of K_{Ca} channels at the application site. In the present study, raising $[K^+]_o$

did indeed produce a hyperpolarization which was entirely abolished by barium and was mediated by functional Kir channels localized to the endothelium in both WKY and SHR rats. These data are consistent with a role for Kir channels in potentiating hyperpolarization in endothelial cells, rather than an action in the smooth muscle cells, as previously reported (Edwards *et al.* 1998). Functional Kir channel activity is also restricted to the endothelium of third order branches of rat mesenteric arteries (Doughty *et al.* 2001; Crane *et al.* 2003).

In both WKY and SHR, there was a more extended plateau region adjacent to the ACh application site when measuring vasodilatation than was the case for membrane potential. That the hyperpolarization is closely related to the vasodilatation has been demonstrated here by the absence of both parameters when the endothelium was disrupted and by the significant linear correlation between the two parameters in all experimental groups. The apparent mismatch in the data at sites close to the ACh application, particularly in WKY, may result from the hyperpolarization being supramaximal, while further along the artery, the reduction in the overall hyperpolarization may lead to a less effective spread of the conducted vasodilatation. In support of this proposal, we found that there was no linear correlation between the two parameters when points in excess of 175 mV•s overall

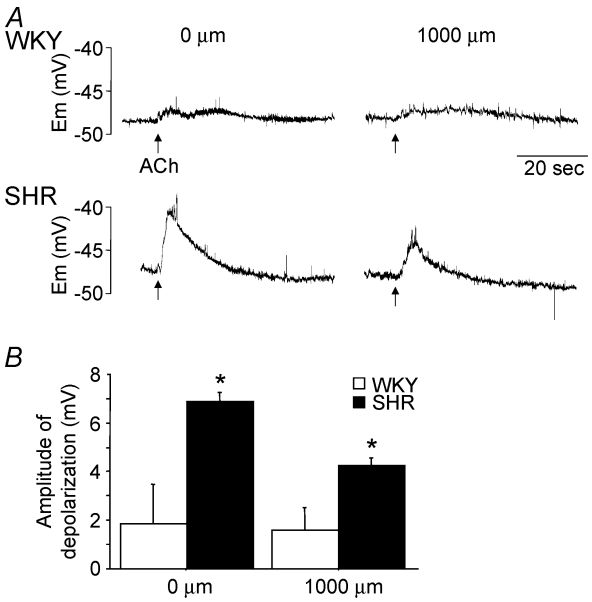

Figure 8. ACh-induced depolarization
Representative tracings (*A*) and summarized data (*B*) of local and conducted depolarization induced by ACh in the presence of apamin (0.5 μmol l^{-1}) plus charybdotoxin (60 nmol l^{-1}). Data are means ± S.E.M.; $n = 6$ in each strain. *$P < 0.05$ *versus* WKY. Representative tracings in each strain were obtained from the same cell. Indomethacin (10 μmol l^{-1}) and L-NAME (100 μmol l^{-1}) present throughout.

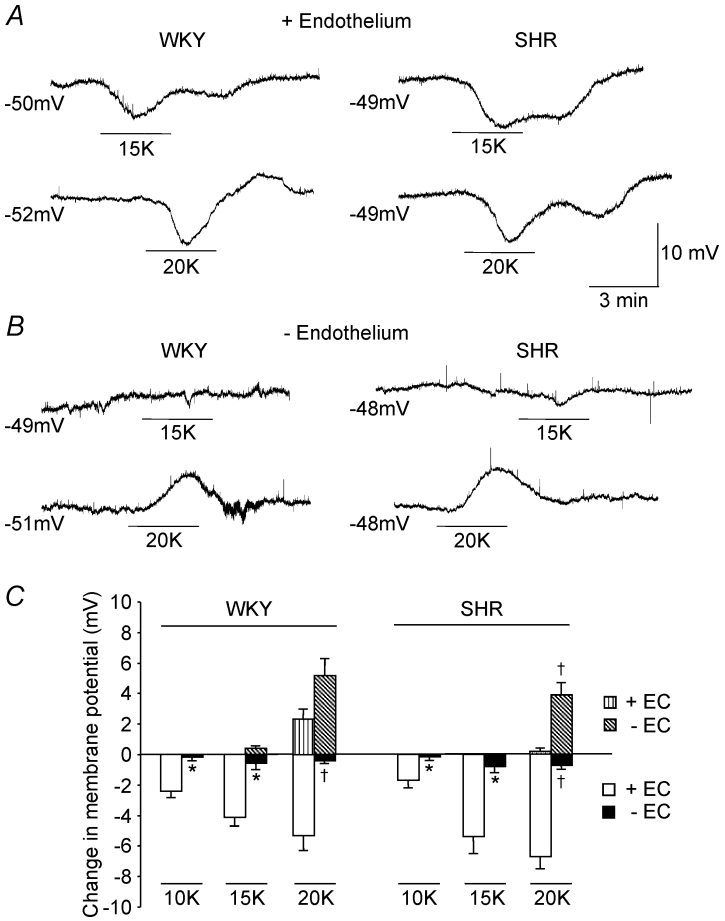

Figure 7. Role of the endothelium in K^+-induced hyperpolarization in WKY and SHR
A, in endothelium-intact arteries, bath applied K^+ (15 or 20 mmol l^{-1}) hyperpolarized the membrane in the two strains. Note that the onset of the hyperpolarization is slow in both strains. *B*, disruption of the endothelium abolished the K^+ (15 or 20 mmol l^{-1})-induced hyperpolarization in both strains. At higher concentration of K^+ (20 mmol l^{-1}), hyperpolarization turned to depolarization in both strains. *C*, summarized data of the membrane potential changes to bath applied K^+ in mesenteric arteries with (+ EC) or without endothelium (– EC) in WKY and SHR. Indomethacin (10 μmol l^{-1}), L-NAME (100 μmol l^{-1}) and nifedipine (1 μmol l^{-1}) present throughout. Data are means ± S.E.M.; $n = 5$–6 in each strain. *$P < 0.05$ *versus* +EC. †$P < 0.01$ *versus* +EC.

hyperpolarization were considered. The reduction in the overall hyperpolarization at the ACh application site in WKY in the presence of barium, without an apparent effect on vasodilatation, is also consistent with this hypothesis.

In contrast to WKY, barium was without effect on conducted responses in SHR. As a consequence, conducted responses were nearly identical between the strains in the presence of barium, suggesting a lack of involvement of Kir channels in conducted vasomotor responses in SHR. In rat cerebral arteries, it has been reported that the Na^+,K^+-ATPase-independent K^+-induced dilatation, probably via Kir channels, is impaired in hypertension (McCarron & Halpern, 1990). Thus, the absence of the effects of barium on conducted responses in mesenteric arteries of SHR could be attributed to an altered sensitivity to K^+ ions. However, such a possibility is unlikely, as K^+-induced hyperpolarization did not differ between the strains and both were sensitive to barium.

Recent studies have shown that Kir2.1 can form functional heteromeric channels in conjunction with Kir2.2 (Zobel *et al.* 2003) and Kir2.4 (Schram *et al.* 2002) and that these channels have properties that differ from those of homomeric channels, such as sensitivity to barium. Consequently, variation in the expression of one or other of the channel subunits could be expected to affect the properties of the Kir channel in tissues in which the subfamily members are coexpressed (Schram *et al.* 2002, 2003). However, using our methods we could find no evidence for any difference in the mRNA expression of the Kir2.0 genes within intact mesenteric

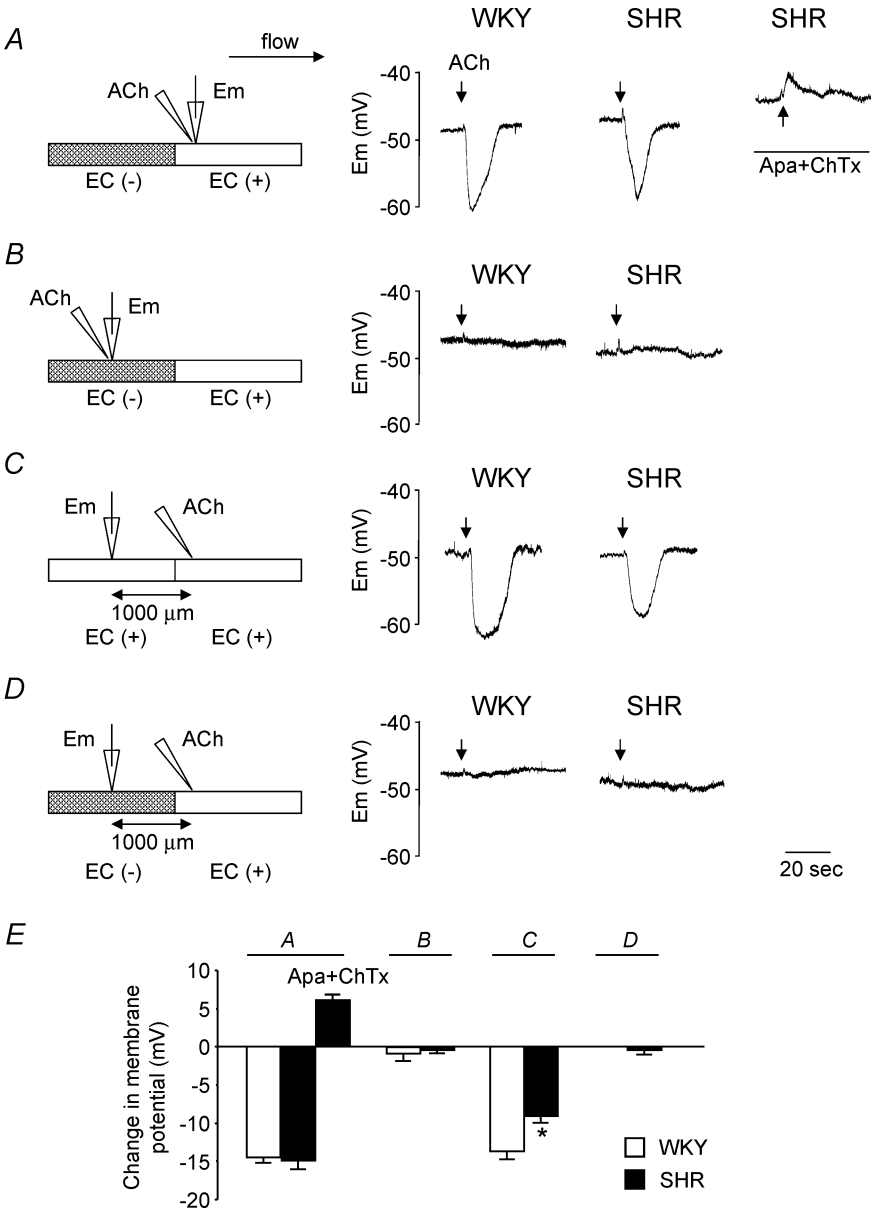

Figure 9. Role of the endothelium in generation and conduction of ACh-induced responses
In the endothelium-intact half of the artery, ACh produced both local (*A*) and conducted (*C*) responses in the two strains. In the endothelium-disrupted half of the artery, neither local (*B*) nor conducted (*D*) responses were observed in both strains. *E*, summarized data. Indomethacin (10 μmol l^{-1}) and L-NAME (100 μmol l^{-1}) present throughout. ACh-induced depolarization was obtained in the presence of apamin (Apa, 0.5 μmol l^{-1}) plus charybdotoxin (ChTx, 60 nmol l^{-1}). Data are means ± S.E.M.; $n = 5$ (*A*, *B* and *D*) and $n = 7$ (*C*) in each strain. $^*P < 0.05$ *versus* WKY. Experiments in *A*, *B* and *D* were conducted in the same arteries.

arteries of these rat strains. Quantitative PCR was used to show that mRNA encoding Kir2.2 is the predominantly expressed Kir2.0 subtype in the mesenteric artery. Because arteries are composed of multiple layers of smooth muscle cells and only a single layer of endothelial cells it is tempting to speculate that Kir2.2 is expressed mainly in the smooth muscle layer whilst Kir2.1 and Kir2.4 are expressed in the endothelium. The presence of Kir2.2 in the smooth muscle would not be in conflict with our results of a lack of effect of K^+ ions following disruption of the endothelium since Kir2.2 channels are rapidly inactivated at hyperpolarizing potentials (Takahashi *et al.* 1994). In contrast to our study, Bradley *et al.* (1999) have reported the expression of mRNA for Kir2.1, but not Kir2.2 or Kir2.3, in cultured myocytes derived from the mesenteric artery of 12–14 week Sprague-Dawley rats. This may suggest that further differences in Kir2.0 gene expression arise under *in vitro* conditions. It is important to understand the relationships that exist between gene transcription, mRNA processing and translation, post-translational modification and processing, protein expression and function, channel assembly and trafficking and most importantly, the function and physiological outcome *in vivo*. We have examined the first and the final steps in this complex process, namely mRNA expression of Kir2.0 genes and the function of Kir channels in the mesenteric arteries of WKY and SHR and can find no evidence supporting a difference in Kir channel expression or function.

Given that conduction of responses relies on gap junctions (Segal & Duling, 1989), one might expect that changes in the number of endothelial gap junctions would impact on conduction. Indeed, it has been reported that conduction of vasodilatation is impaired in Cx40-deficient mice (de Wit *et al.* 2000; Figueroa *et al.* 2003). In the present study, expression of Cx37, but not Cx40 and Cx43, was significantly less in the endothelium of the mesenteric artery of SHR compared to WKY. However, decreased

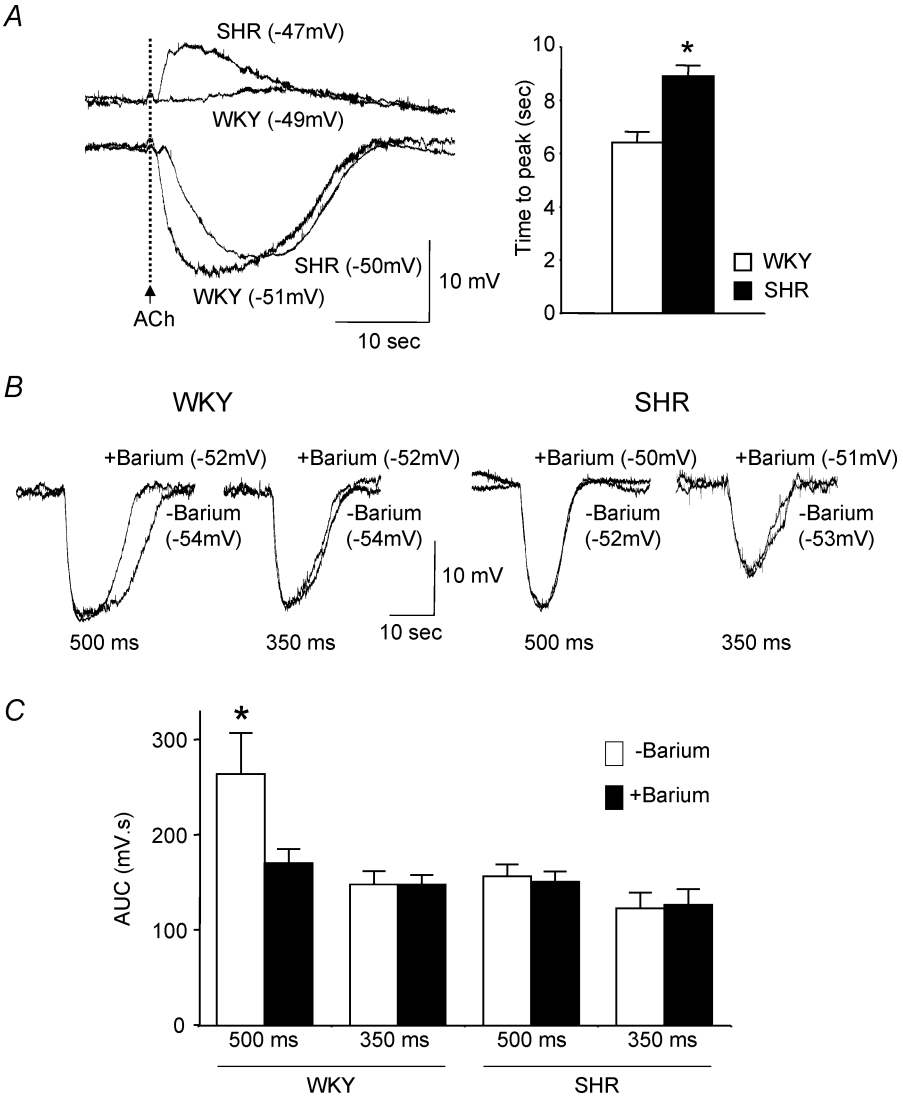

Figure 10. Role of hyperpolarization in the activation of Kir channels at the site of ACh application
A, ACh-induced depolarization in SHR (upper panel), coincided with the ACh-induced hyperpolarization (lower panel) which was slower in SHR than the hyperpolarization in WKY. The time from ACh application to the peak hyperpolarization (Time to peak) was significantly longer in SHR compared to WKY. Data are means ± S.E.M.; $n = 22$ in each strain. $^*P < 0.01$ *versus* WKY. Upper traces were recorded in the presence of apamin and charybdotoxin. Representative tracings in each strain were obtained from the same cell. Representative tracings (*B*) and summarized data (*C*) of the effect of barium (30 μM) on the overall hyperpolarization in WKY and SHR. In WKY, overall hyperpolarization to ACh (500 ms) was diminished by barium. When the ACh stimulus was shorter (350 ms), the overall hyperpolarization was significantly reduced and barium had no further effect. In SHR, the overall hyperpolarization was significantly smaller than in WKY (500 ms) and barium was without effect. Data are means ± S.E.M.; $n = 7$ (500 ms WKY, SHR) and 5 (350 ms WKY, SHR). $^*P < 0.05$ *versus* all the other groups. Indomethacin (10 μmol l^{-1}) and L-NAME (100 μmol l^{-1}) present throughout. The figures in parentheses indicate the resting membrane potential for that recording.

Cx37 expression does not explain the strain difference in conducted vasomotor responses observed in the present study, since this strain difference was no longer detected in the presence of barium. The reason for the inability of the decreased endothelial Cx37 expression to alter conducted responses in SHR is not known. The extent of the reduction in Cx37 expression, observed in the present study, may not be sufficient to have an effect. Alternatively, Cx37 may not play a role in the conduction of vasomotor responses. This notion may be supported by findings that conducted vasodilatation to ACh is unchanged in cremaster arterioles of Cx37-deficient mice (Kumer *et al.* 1998). Further studies are needed to clarify these issues.

After blockade of EDHF-mediated hyperpolarization with apamin plus charybdotoxin, iontophoresed ACh produced a depolarization which was considerably larger in SHR than WKY. This depolarization spread to distant sites in both strains. Like the hyperpolarization, the depolarization arose from and was conducted within the endothelium. In hypertension, the production of cyclooxygenase-dependent endothelium-derived contracting factors, such as thromboxane A2 and prostaglandin H2, is augmented (Lüscher *et al.* 1992). However, these factors cannot account for the depolarization reported here, since the cyclooxygenase inhibitor indomethacin was present in all experiments. While the nature of the depolarization in SHR is not clear from the present study, the coincidence of the depolarization with the hyperpolarization suggests that the depolarization may act to reduce the duration of the hyperpolarization and the consequent activation of Kir channels in the vicinity of the stimulus. Indeed, the overall hyperpolarization in SHR

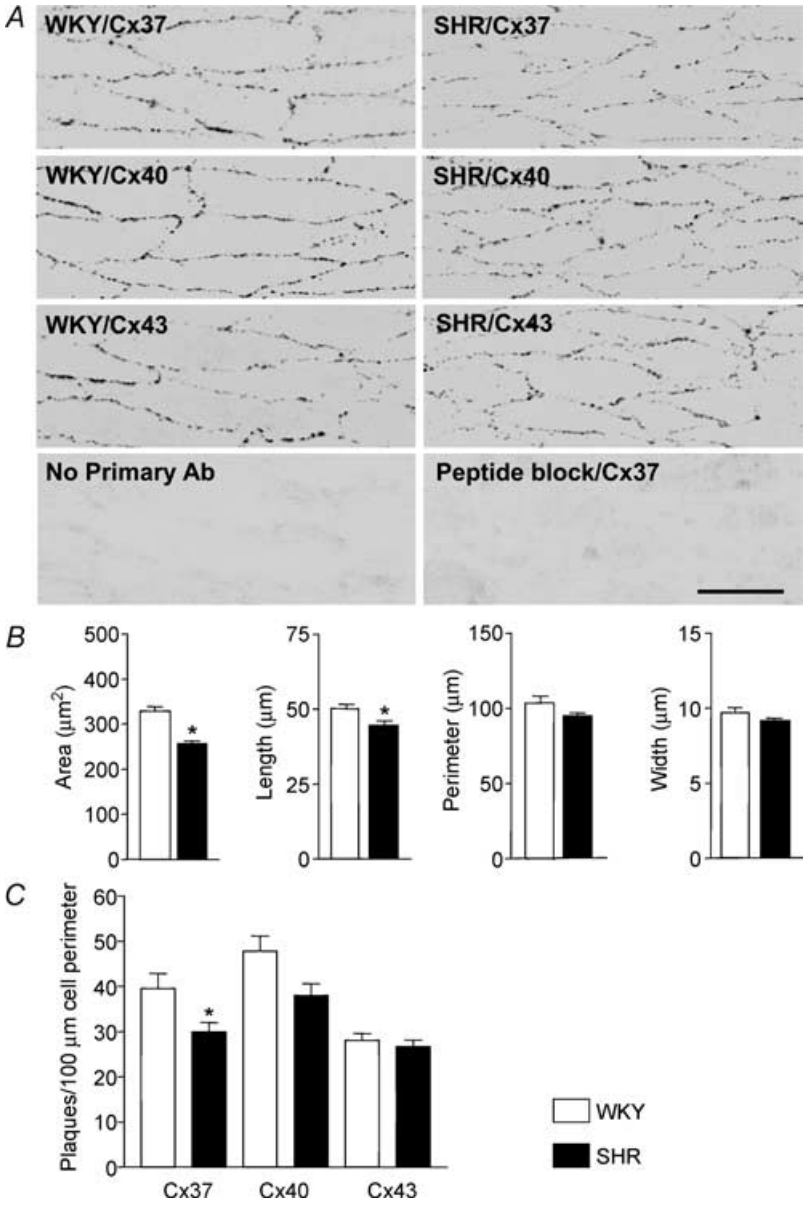

Figure 11. Cx protein expression in mesenteric arteries of WKY and SHR
A, the endothelium, viewed *en face*, is labelled with antibodies to Cx37, 40 and 43. Labelling is evident along the perimeter of endothelial cells in both strains. Bottom panels show the absence of staining when the primary antibody was omitted (No primary Ab) or when the primary antibody was pre-incubated with the antigenic peptide (Peptide block/Cx37). Calibration bar = 20 μm. *B*, morphology of endothelial cells in WKY and SHR mesenteric arteries as determined from immunohistochemical labelling of Cx37. *C*, density of protein expression for Cxs 37, 40, and 43 in the endothelium of WKY and SHR mesenteric arteries. Data are expressed as the number of Cx plaques per 100 μm of endothelial cell perimeter. Data are means ± S.E.M.; $n = 4$ in each strain. $^*P < 0.05$ *versus* WKY.

was reduced at the site of ACh application compared to WKY and there was no evidence for the activation of Kir channels. In further support for this hypothesis, a reduction in the duration of the hyperpolarization in the mesenteric arteries from WKY rats following a decrease in the ACh stimulus resulted in a failure to activate Kir channels.

In conclusion, the present study provides evidence for involvement of Kir channels in the generation of conducted vasomotor responses and a lack of this involvement during hypertension. This novel finding is of clinical importance, since the absence of Kir channel activation could increase peripheral resistance, thereby contributing to the maintenance and/or development of hypertension. Indeed, it has been reported that barium increases vascular resistance in human forearm resistance vessels *in vivo* (Dawes *et al.* 2002). The detailed mechanisms underlying the endothelium-dependent depolarization and its interaction with hyperpolarization warrants further investigation, since this may represent a novel therapeutic strategy to counteract the impairment of vasomotor responses during hypertension.

References

Bradley KK, Jaggar JH, Bonev AD, Heppner TJ, Flynn ERM, Nelson MT & Horowitz B (1999). $K_{ir}2.1$ encodes the inward rectifier potassium channel in rat arterial smooth muscle cells. *J Physiol* **515**, 639–651.

Coleman HA, Tare M & Parkington HC (2001). K^+ currents underlying the action of endothelium-derived hyperpolarizing factor in guinea-pig, rat and human blood vessels. *J Physiol* **531**, 359–373.

Crane GJ, Neild TO & Segal SS (2004). Contribution of active membrane processes to conducted hyperpolarization in arterioles of hamster cheek pouch. *Microcirculation* **11**, 425–433.

Crane GJ, Walker SD, Dora KA & Garland CJ (2003). Evidence for a differential cellular distribution of inward rectifier K channels in the rat isolated mesenteric artery. *J Vasc Res* **40**, 159–168.

Dawes M, Sieniawska C, Delves T, Dwivedi R, Chowienczyk PJ & Ritter JM (2002). Barium reduces resting blood flow and inhibits potassium-induced vasodilation in the human forearm. *Circulation* **105**, 1323–1328.

Doughty JM, Boyle JP & Langton PD (2001). Blockade of chloride channels reveals relaxations of rat small mesenteric arteries to raised potassium. *Br J Pharmacol* **132**, 293–301.

Duling BR & Berne RM (1970). Propagated vasodilation in the microcirculation of the hamster cheek pouch. *Circ Res* **26**, 163–170.

Edwards G, Dora KA, Gardener MJ, Garland CJ & Weston AH (1998). K^+ is an endothelium-derived hyperpolarizing factor in rat arteries. *Nature* **396**, 269–272.

Emerson GG, Neild TO & Segal SS (2002). Conduction of hyperpolarization along hamster feed arteries: augmentation by acetylcholine. *Am J Physiol* **283**, H102–H109.

Emerson GG & Segal SS (2000). Endothelial cell pathway for conduction of hyperpolarization and vasodilation along hamster feed artery. *Circ Res* **86**, 94–100.

Figueroa XF, Paul DL, Simon AM, Goodenough DA, Day KH, Damon DN & Duling BR (2003). Central role of connexin40 in the propagation of electrically activated vasodilation in mouse cremasteric arterioles in vivo. *Circ Res* **92**, 793–800.

Fujii K, Tominaga M, Ohmori S, Kobayashi K, Koga T, Takata Y & Fujishima M (1992). Decreased endothelium-dependent hyperpolarization to acetylcholine in smooth muscle of the mesenteric artery of spontaneously hypertensive rats. *Circ Res* **70**, 660–669.

Goto K, Fujii K, Kansui Y, Abe I & Iida M (2002). Critical role of gap junctions in endothelium-dependent hyperpolarization in rat mesenteric arteries. *Clin Exp Pharmacol Physiol* **29**, 595–602.

Goto K, Fujii K, Onaka U, Abe I & Fujishima M (2000). Renin-angiotensin system blockade improves endothelial dysfunction in hypertension. *Hypertension* **36**, 575–580.

Griffith TM, Chaytor AT, Taylor HJ, Giddings BD & Edwards DH (2002). cAMP facilitates EDHF-type relaxations in conduit arteries by enhancing electrotonic conduction via gap junctions. *Proc Natl Acad Sci U S A* **99**, 6392–6397.

Harder DR (1984). Pressure-dependent membrane depolarization in cat middle cerebral artery. *Circ Res* **55**, 197–202.

Hill CE, Eade J & Sandow SL (1999). Mechanisms underlying spontaneous rhythmical contractions in irideal arterioles of the rat. *J Physiol* **521**, 507–516.

Hill CE, Phillips JK & Sandow SL (2001). Heterogenous control of blood flow amongst different vascular beds. *Med Res Rev* **21**, 1–60.

Hoepfl B, Rodenwaldt B, Pohl U & de Wit C (2002). EDHF, but not NO or prostaglandins, is critical to evoke a conducted dilation upon ACh in hamster arterioles. *Am J Physiol* **283**, H996–H1004.

Horiuchi T, Dietrich HH, Hongo K & Dacey RG Jr (2002). Mechanism of extracellular K^+-induced local and conducted responses in cerebral penetrating arterioles. *Stroke* **33**, 2692–2699.

Kansui Y, Fujii K, Nakamura K, Goto K, Oniki H, Abe I, Shibata Y & Iida M (2004). Angiotensin II receptor blockade corrects altered expression of gap junctions in vascular endothelial cells from hypertensive rats. *Am J Physiol* **287**, H216–H224.

Kumer SC, Simon AM, Paul DL, Burt J & Duling BR (1998). Connexin 37 is involved in the conducted vasomotor response of arterioles. *FASEB J* **12**, A37.

Lüscher TF, Boulanger CM, Dohi Y & Yang ZH (1992). Endothelium-derived contracting factors. *Hypertension* **19**, 117–130.

McCarron JG & Halpern W (1990). Impaired potassium-induced dilation in hypertensive rat cerebral arteries does not reflect altered Na^+, K^+-ATPase dilation. *Circ Res* **67**, 1035–1039.

Neild TO (1989). Measurement of arteriole diameter changes by analysis of television images. *Blood Vessels* **26**, 48–52.

Oishi H, Schuster A, Lamboley M, Stergiopulos N, Meister JJ & Beny JL (2002). Role of membrane potential in vasomotion of isolated pressurized rat arteries. *Life Sci* **71**, 2239–2248.

Quayle JM, Nelson MT & Standen NB (1997). ATP-sensitive and inwardly rectifying potassium channels in smooth muscle. *Physiol Rev* **77**, 1165–1232.

Rivers RJ, Hein TW, Zhang C & Kuo L (2001). Activation of barium-sensitive inward rectifier potassium channels mediates remote dilation of coronary arterioles. *Circulation* **104**, 1749–1753.

Rummery NM, Hickey H, McGurk G & Hill CE (2002*b*). Connexin37 is the major connexin expressed in the media of caudal artery. *Arterioscler Thromb Vasc Biol* **22**, 1427–1432.

Rummery NM, McKenzie KU, Whitworth JA & Hill CE (2002*a*). Decreased endothelial size and connexin expression in rat caudal arteries during hypertension. *J Hypertens* **20**, 247–253.

Sandow SL, Goto K, Rummery NM & Hill CE (2004). Developmental changes in myoendothelial gap junction mediated vasodilator activity in the rat saphenous artery. *J Physiol* **556**, 875–886.

Sandow SL & Hill CE (2000). Incidence of myoendothelial gap junctions in the proximal and distal mesenteric arteries of the rat is suggestive of a role in endothelium-derived hyperpolarizing factor-mediated responses. *Circ Res* **86**, 341–346.

Sandow SL, Looft-Wilson R, Doran B, Grayson TH, Segal SS & Hill CE (2003). Expression of homocellular and heterocellular gap junctions in hamster arterioles and feed arteries. *Cardiovascular Res* **60**, 643–653.

Sandow SL, Tare M, Coleman HA, Hill CE & Parkington HC (2002). Involvement of myoendothelial gap junctions in the actions of endothelium-derived hyperpolarizing factor. *Circ Res* **90**, 1108–1113.

Schram G, Melnyk P, Pourrier M, Wang Z & Nattel S (2002). Kir2.4 and Kir2.1 K^+ channel subunits co-assemble: a potential new contributor to inward rectifier current heterogeneity. *J Physiol* **544**, 337–349.

Schram G, Pourrier M, Wang Z, White M & Nattel S (2003). Barium block of Kir2 and human cardiac inward rectifier currents: evidence for subunit-heteromeric contribution to native currents. *Cardiovascular Res* **59**, 328–338.

Segal SS (2001). Endothelium and smooth muscle pathways for conduction along resistance microvessels. In *EDHF 2000*, ed.Vanhoutte PM, pp. 22–31. Taylor & Francis, London.

Segal SS & Duling BR (1989). Conduction of vasomotor responses in arterioles: a role for cell-to-cell coupling? *Am J Physiol* **256**, H838–H845.

Sobey CG (2001). Potassium channel function in vascular disease. *Arterioscler Thromb Vasc Biol* **21**, 28–38.

Takahashi N, Morishige K, Jahangir A, Yamada M, Findlay I, Koyama H & Kurachi Y (1994). Molecular cloning and functional expression of cDNA encoding a second class of inward rectifier potassium channels in the mouse brain. *J Biol Chem* **269**, 23274–23279.

Takano H, Dora KA, Spitaler MM & Garland CJ (2004). Spreading dilatation in rat mesenteric arteries associated with calcium-independent endothelial cell hyperpolarization. *J Physiol* **556**, 887–903.

Welsh DG & Segal SS (2000). Role of EDHF in conduction of vasodilation along hamster cheek pouch arterioles in vivo. *Am J Physiol* **278**, H1832–H1839.

de Wit C, Roos F, Bolz SS, Kirchhoff S, Kruger O, Willecke K & Pohl U (2000). Impaired conduction of vasodilation along arterioles in connexin40-deficient mice. *Circ Res* **86**, 649–655.

Yamamoto Y, Fukuta H, Nakahira Y & Suzuki H (1998). Blockade by 18beta-glycyrrhetinic acid of intercellular electrical coupling in guinea-pig arterioles. *J Physiol* **511**, 501–508.

Yamamoto Y, Klemm MF, Edwards FR & Suzuki H (2001). Intercellular electrical communication among smooth muscle and endothelial cells in guinea-pig mesenteric arterioles. *J Physiol* **535**, 181–195.

Zobel C, Cho HC, Nguyen T-T, Pekhletski R, Diaz RJ, Wilson GJ & Backx PH (2003). Molecular dissection of the inward rectifier potassium current (I_{K1}) in rabbit. cardiomyocytes: evidence for heteromeric co-assembly of $K_{ir2.1}$ and $K_{ir2.2}$. *J Physiol* **550**,. 365–372.

Acknowledgements

We thank the National Heart Foundation of Australia and National Health and Medical Research Council of Australia for financial support.